ALBA BOOSTER SETTINGS FOR AN OPTIMIZED PERFORMANCE

G. Benedetti, D. Einfeld, J. Marcos, M. Muñoz, M. Pont
CELLS, Ctra. BP-1413, Km 3.3, Cerdanyola, Spain.

Abstract

The ALBA booster is a 100 MeV-3 GeV synchrotron, with large circumference of 249.6 m and low emittance of 9 nm·rad, cycling at 3 Hz. The ring consists of a 4-fold symmetric modified FODO lattice with defocusing gradient dipoles. Magnetic measurements on all magnets have been performed. Their evaluation, the studies and the lattice settings to recover the design optics preserving good machine performances, such as the lattice flexibility, the low beta functions and large dynamic apertures at high chromaticities, are described.

INTRODUCTION

The ALBA booster layout consists of a modified FODO lattice based on alternating defocusing gradient dipoles and focusing quadrupoles [1]. The combined dipoles (BM05, BM10) and the quadrupole family of the unit cell (QH02) have also a built-in sextupole component in the iron pole profile to correct the natural chromaticity.

The magnetic field in all the magnets has been measured in 2008. All the magnets were found within the specifications except the family of so called long dipoles, where the edge vertical focusing resulted in a gradient lower than expected due to a error in the evaluation of the end chamfer cut in the pre-series (Fig. 1). The sextupole terms in the combined dipoles and quadrupoles were also accurately measured, including the fringing regions. The impact of the measured sextupole terms was simulated and the correction of the chromaticity with the sextupoles families optimized all along the energy ramping in order to preserve a good dynamic aperture and minimizing their strength.

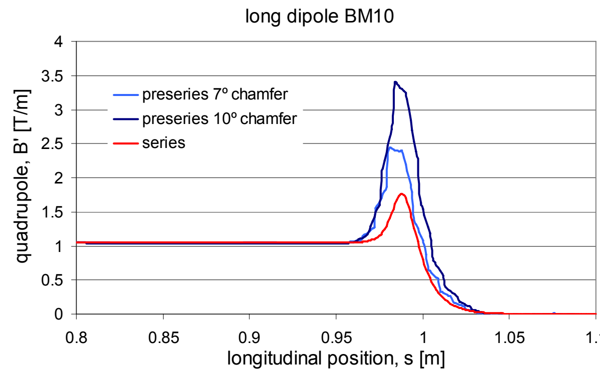

Figure 1: The quadrupole profile in the fringing region of the long dipole. The peak value measured on the series (red line) is about a factor two below the needed value (chamfer cut between 7° and 10°).

MAGNETIC MEASUREMENTS

The two dipole families have been measured at CELLS with a special Hall probe bench designed to precisely scan the magnetic field in the fringing region up to 200 mm inside the iron gap. Magnetic measurements have been performed at several currents covering all the energy ramping from 100 MeV to 3 GeV. The obtained field maps have been completed with the data previously measured inside the magnet by the manufacturer, conveniently scaled.

The particle trajectory is numerically integrated in the field map of each bending magnet in order to have exactly the design bending angle, and the corresponding beam energy is determined.

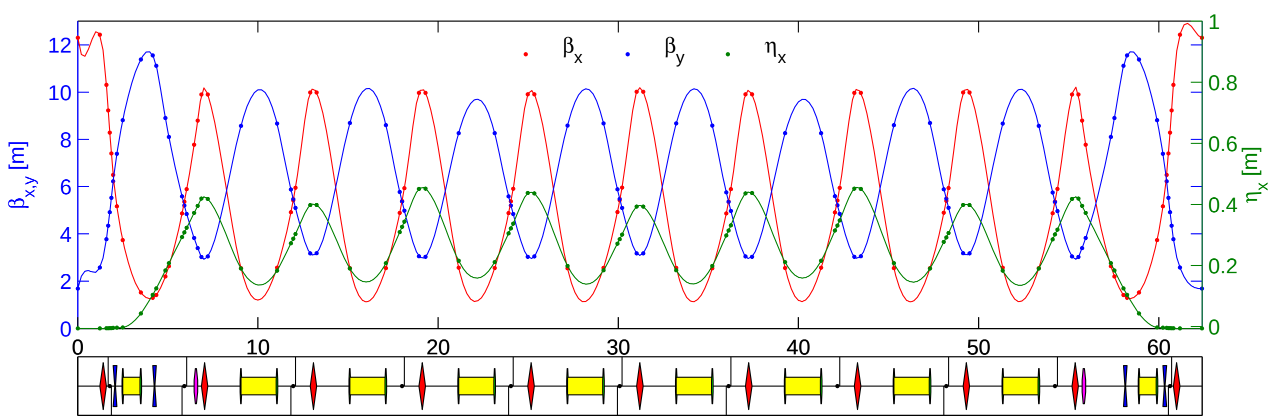

Figure 2: Beta and dispersion functions in one arc of the machine, matched according to the measured magnets. The quadrant composes of 8 unit cells with long dipole and focusing quadrupole, and 2 matching sections with short dipole and three quadrupole families. The sextupole families are located in the dispersive section next to the short dipoles.

Under this condition, the quadrupole and sextupole terms are determined by a 3rd order polynomial fit of the transversal dependence of the field around the beam trajectory.

The variation of the quadrupole and sextupole terms in the dipoles with the beam energy has been measured. The maximum change is at low energy from 100 and 200 MeV. Then correction of tunes and beta functions along the energy ramping has been taken into account.

The quadrupole gradient in the central part agrees very well with the design value and the variation from magnet to magnet is within the specifications, ±0.5%, in both dipole families. The edge focusing gradient in the long dipole family BM10, with bend angle θ = 10°, instead, has been found to be much lower than the design one. The effective pole face rotation results in 1.1° and 1.3°, respectively at 100 MeV and 3 GeV, instead of θ/2 = 5°. This missing term is equivalent to a reduction of 2.2% of the total integrated gradient of the long dipole.

The measured sextupole in the fringing regions results in a contribution of about 20% of the total integrated sextupole term of the magnet.

LATTICE MODEL

A realistic model of the machine has been studied introducing the measured parameters. Several solutions were considered to compensate the missing gradient in the dipoles, and eventually the betas and the tunes are recovered readjusting the four quadrupole families.

Table 1: Long dipole BM10 model parameters. The values at 0.1 GeV are scaled by a factor 30 to be compared with 3 GeV

Parameter	Nominal	Meas 100 MeV	Meas 3 GeV
Magn. length (m)	2.000	2.012	2.005
Bend angle (°)	10	10	10
Quadrupole (T/m)	2.29	2.298	2.291
Sextupole (T/m^2)	18.0	19.5	19.5
Edge focus angle (°)	5.0	1.1	1.3
Integr. edge sext. (T/m)	-	4.4	5.9

Table 2: Short dipole BM05 parameters.

Parameter	Nominal	Meas 100 MeV	Meas 3 GeV
Magn. length (m)	1.000	1.006	1.001
Bend angle (°)	5	5	5
Quadrupole (T/m)	2.29	2.310	2.274
Sextupole (T/m^2)	18.0	18.8	19.7
Edge focus angle (°)	2.5	2.5	1.9
Integr. edge sext. (T/m)	-	5.0	5.75

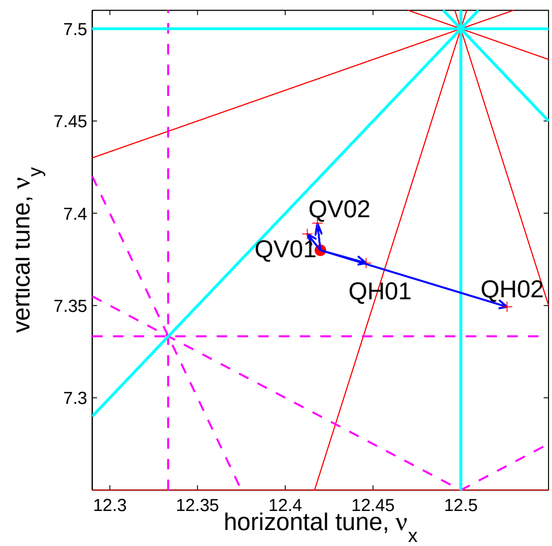

Figure 3: Nominal working point (12.42, 7.38) and tune shifts due to a strength change Δk = 0.01 in the four quadrupole families. The resonance lines up to 4th order are plotted.

Dipoles

The modelling parameters inferred from the magnetic measurements on the dipole magnets at 100 MeV and 3 GeV are listed in Tables 1 and 2.

The missing gradient at the edges results in a shift of the vertical tune from 7.38 to 7.12.

The dipoles are modelled using a hard-edge model [2].

Quadrupoles

The nominal working point is recovered increasing by 30% the strength of one of the defocusing quadrupole families in the matching section (QV01). The betas are then readjusted with small changes in the four quadrupole families.

The lattice flexibility is preserved and the tunes can be changed up to ±0.5 units in both planes with small changes in the beta functions. Figure 3 shows the response on the tunes to each quadrupole family.

Sextupoles

The sextupole terms of the combined dipole and quadrupole families are included in the model, both in the central and in the edge regions. In the nominal design, the sextupole terms corrected the chromaticity to (+1, +1) at injection and extraction.

Including in the model the measured sextupoles, the chromaticities are not positive any more (Table 3). Therefore, the two sextupoles families are used also at injection and extraction in order to avoid the head-tail instability. The sextupole in the dipoles is modelled as a homogeneous term in the body plus two thin lenses located at the edges. The contribution of the fringing sextupoles to the chromaticity can not be neglected since it is of 5 units in the vertical plane.

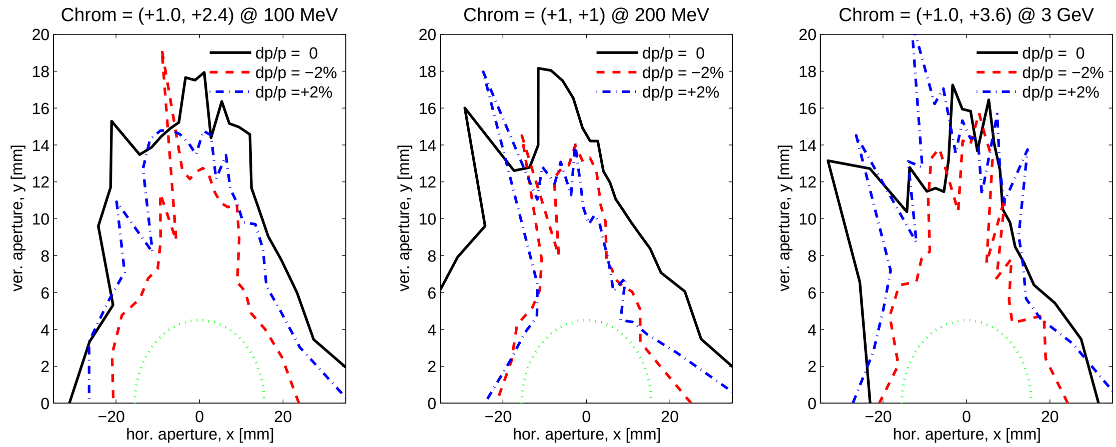

Figure 4: Dynamic apertures compared with the vacuum chamber physical acceptance at injection (leftmost), maximum eddy current effect (centre), and extraction (rightmost).

Table 3: Chromaticities (ξ_x, ξ_y) with the nominal design magnets compared those calculated with the measured sextupole terms in the dipoles. The fringing contribution gives about 4-5 units in the vertical plane.

Energy	Design Chrom.	Meas. without fringing	Meas. with fringing
0.1 GeV	(+1, +1)	(-0.2, -0.5)	(-1.4, +3.4)
3.0 GeV	(+1, +1)	(-0.7, -0.3)	(-2.2, +4.9)

RAMPING AND EDDY CURRENTS

Correction of the chromaticity with the two dedicated sextupole families, SH and SV, is calculated with the measured sextupoles terms in the dipoles.

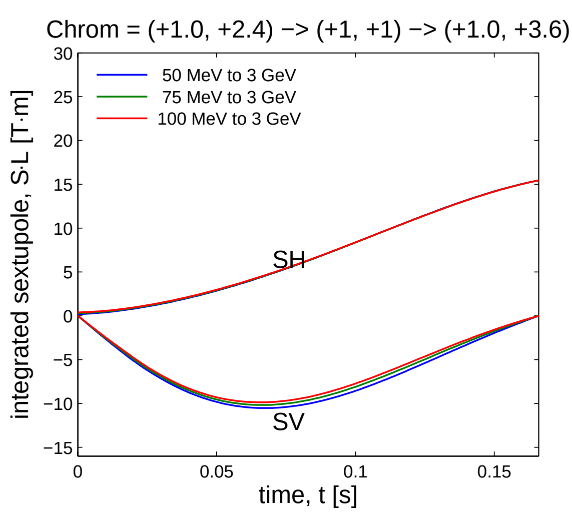

Figure 5: The SH and SV sextupole tracking with dipole ramping starting at different energies. The sextupole power supplies tracking to keep the chromaticities higher than +1 is performed in the minimum range in order to have the largest dynamic aperture all along the ramping.

An optimized solution for the sextupole waveforms is chosen to have the largest dynamic aperture all along the ramping with positive chromaticity to avoid head-tail instability. This condition is fulfilled injecting at 100 MeV with chromaticity corrected to (+1.0, +2.4), going to (+1.0, +1.0) at 200 MeV where the eddy current effect is maximum, and extracting at 3 GeV at (+1.0, +3.6). In this way the used sextupole strength is minimized all along the ramping.

Figure 4 shows the dynamic apertures on-energy and ±2% off-energy with the three lattices corresponding at 100 MeV, 200 MeV and 3 GeV.

The sextupole waveforms are calculated also for dipole ramping starting at energy lower than 100 MeV (Fig. 5). In this case the injection is performed with a time delay (“injection on the fly”) at a point with higher energy slope in order that the beam stays less time at low energy, where the damping and lifetime are worse. The disadvantage is having larger eddy currents at lower energy, which gives some reduction in the dynamic aperture and in the dynamic energy acceptance.

ACKNOWLEDGEMENTS

Z. Martí is appreciated for useful suggestions and for the dynamic aperture function developments with AT.

REFERENCES

[1] G. Benedetti et al., “Optics for the ALBA Booster Synchrotron”, EPAC’08, Genoa, June 2008.
[2] D. Einfeld et al. “Modelling of gradient bending magnets for the beam dynamics studies at ALBA”, PAC’07, Albuquerque, May 2007.
[3] G. Benedetti, “Sextupoles and eddy currents in the Booster”, CELLS internal report, AAD-BO-BD-AN-137, 2006.